Environ Geochem Health (2023) 45:629–645
https://doi.org/10.1007/s10653-022-01232-w

ORIGINAL PAPER

Potentially toxic elements in smoke particles and residual ashes by biomass combustion from Huangshi National Mine Park, China

Yanyan Liu · Xiaochun Ye · Bingwei Zhou · Zhitao Tian · Caiying Liu · Kaiyuan Li

Received: 19 August 2021 / Accepted: 16 February 2022 / Published online: 10 March 2022

Abstract This paper investigates the fractional and spatial distribution characteristics of potentially toxic elements (PTEs) in smoke particles and residual ashes from mine-park-biomass combustion. It then evaluates the consequential potential environment risk by using a Geo-accumulation index and Nemerow pollution index methods. Biomass combustibles are comprised of *Camphor leaves* (*CL*), *Camphor dead-branch* (*CB*), *Ramie* (*RA*), *Miscanthus sinensis* (*MS*), and *Dryopteris* (*DR*). The results show that the products of combustion contain PTEs, As, Cr, Cu, and Zn, etc. Among them, the content of As, Cr, Cu, Pb elements in smoke particles of *CB* was higher than other combustibles. Moreover, Cr, Mn, Ni, and Pb in residual ashes of *CL* were higher than others. The proportion of acid-soluble and reducible fraction of As in residual ash was higher, while Cr existed mainly in the oxidizable and residual fraction. Besides, the available state of As gradually decreased from 74% (400 °C) to 41% (800 °C), indicating that the increase of temperature significantly reduced the bioavailability of As. Meanwhile, with the increase of temperature, the concentration of PTEs in smoke particles decreased and PTEs in residual ashes increased in different degrees. The risk evaluation results indicate that PTEs may cause moderate or higher levels of contamination. The overall contamination level of PTEs in the residual ashes of *CB* was higher than that of other plant. The results show in this study would contribute to understanding the environmental risks of wildfire and prescribed burning in PTEs-contaminated areas.

Keywords Contaminated biomass · Potentially toxic elements · Forest fire · Transformation · Fractional distribution · Risk evaluation

Introduction

Potentially toxic elements (PTEs) in the environment, such as As, Co, Cr, Cd, Cu, Ni, Pb, Sb, and Zn, are of broad concern due to their high toxic potential, environmental persistence and tendency to be bio-accumulated (Campos et al., 2015, 2016; Duffus, 2001; Hodson, 2004; Kelly et al., 2006). PTEs contribute to contamination in soil and aquatic environments and the immediate risks to human and ecosystems health. When the body is exposed to PTEs continuously, it may lead to harmful health effects such as stunted physical development, gastrointestinal–kidney–respiratory disorders, anemia, cancer, and so on. (Chen et al., 1996;

Supplementary Information The online version contains supplementary material available at https://doi.org/10.1007/s10653-022-01232-w.

Y. Liu (✉) · X. Ye · B. Zhou · Z. Tian · C. Liu · K. Li
School of Safety Science and Emergency Management, Wuhan University of Technology, Wuhan 430070, Hubei, China
e-mail: wulengheiyin@whut.edu.cn

Pearce et al., 2012; Zhang et al., 2019). A survey conducted by China's Ministry of Environmental Protection and the Ministry of Land and Resources (CEPM & BLR, 2014) shows that soil pollution is serious in some areas, especially in abandoned industrial and mining areas. The over-standard rates of Cd, Hg, As, Cu, Pb, Cr, Zn, and Ni were 7.0%, 1.6%, 2.7%, 2.1%, 1.5%, 1.1%, 0.9%, and 4.8%, respectively. Metal mining is one of the primary anthropogenic sources of PTEs contamination in China, which has proven mineral resource reserves accounting to 12% of the world's total mineral resource (Hu et al., 2011). Mining activities such as mining, milling, and grinding operations, disposal of tailings, and mine and mill waste water change the environments of the original land. That will lead to severe contamination in the mine area, thus causing the accumulation of PTEs in the plant, soil, and aquatic environments of the corresponding area (Dudka & Adriano, 1997; Liu et al., 2005; Yao-Guo et al., 2010; Zhang et al., 2019).

Moreover, the contamination of mine legacy is considered among the worst environmental problems and a serious hazard to ecosystem and human health. The improvement of hostile environment is necessary for ecological restoration of mine legacy (Gutiérrez et al., 2016). Application of suitable plant species for the restoration of mining sites is one of the primary way of ecological restoration (Burges et al., 2018; McCutcheon & Schnoor, 2003; Ranđelović et al., 2016). For example, Huangshi National Mine Park in China with various vegetation plays a significant role in ecological reconstruction, which greatly improved the environment of the mining legacy. Because forest ecosystems can fix most metals in ground biomass and the soil organic layers (especially Hg, Cu, and Pb), thus effectively reducing PTEs mobilization (Shcherbov, 2012). For example, Grigal (2003) reported that around 90% of the Hg in the forest is found to be fixed with soil organic matter (SOM). However, when a wildfire or controlled fire, combustion of biomass and SOM will change soil properties, releasing PTEs to forest ecosystems. Therefore, forest fire is not only the most common disturbance factor in nature but also the main promoting factor of PTEs mobilization in nature (Abraham et al., 2017). Nowadays, fire intensity and frequency have also gradually increased due to climate change. It was reported that approximately 1% world's forests had been affected by fire each year (Barbero et al., 2015; Fraser & Li, 2002).

Forest fire may re-release PTEs from the biomass to the soil surface by biomass combustion and the decomposition of metal complex organic matter in the soil at high temperatures. Alternatively, the interaction of residual ashes with the soil surface leads to re-deposition of PTEs, all of which processes may lead to PTEs change in the soil and thus alter the soil chemical properties (Campos et al., 2016; Jakubus et al., 2010; Ulery et al., 1993). Young and Jan (1977) studied the possibility of metal reactivation after fire in Angel National Forest in California, USA, and found that the concentrations of nine metals increased in ash deposited on the surface. Abraham et al. (2018) reported that As, Cd, Mn, Ni, and Zn contents increased 1.1, 1.6, 1.7, 1.1, and 1.9 times, respectively, in the post-fire environment, whereas the contents of Hg, Cr, and Pb decreased to 0.7, 0.9, and 0.9 times, respectively, highlighting considerable PTEs mobilization during and after a controlled fire. In addition, the presence of PTEs in residual ash is related directly to vegetation type (Beda, 2010; Campos et al., 2015; Shin et al., 2002). For example, Shin et al. (2002) found that the post-fire ash of red pine species contained a high concentration of Cd in the mountainous areas of Korea. Campos et al. (2015) found that Co and Ni contents in the ash of *pine* plantations after the fire were higher than that of *eucalyptus*. Many types of research showed that the high Mn content in ash is related to the typically high Mn content in vegetation, especially in the needles of resinous tree (Abraham et al., 2017; Marco et al., 2005). Besides, some of the PTEs that are volatile at high temperatures may be released into the atmosphere along with the large amount of smoke produced by combustion, and then migrate with atmospheric movement to areas outside the burned area, thus expanding the potential active range of PTEs (Shcherbov, 2012). Meanwhile, forest fire could form a temporary hydrophobic layer on the soil surface or its adjacent areas, resulting in a decrease in soil infiltration levels and an enhancement of surface runoff. As a result, PTEs in residual ash can contaminate downstream waters through surface runoff (Costa et al., 2014; DeBano, 2000; Ebel & Moody, 2017; Moody et al., 2009).

Forest fires and the widespread usage of biomass energy can lead to the mobilization of PTEs fixed in

the contaminated biomass, which is particularly pertinent to legacy mining areas (Abraham et al., 2018; Murphy et al., 2020). Because the soil and biomass of legacy mining areas were contaminated. Therefore, the release and risk of PTEs after fire event in mine-woodlands and mine-park need to be further explored. What about the risk of mobilization of plant-fixed PTEs by fire events (wildfires or controlled burns)? In this study, the total content and distribution of PTEs in fire smoke particles and residual ashes are investigated from laboratory-based combustion of five plant types collected in Huangshi National Mine Park, Hubei Province, China. The main work includes (1) determination of the effects of the temperature and plant type on PTEs concentration and distribution and (2) understanding the environmental risk of biomass combustion in areas with high background value of PTEs. The result will also be helpful for local, city, and national authorities and environmental agencies to conduct better environment and fire management practices within legacy mining landscapes. Moreover, this study may also assist un-rehabilitated mine site management in other fire-prone regions or countries. Despite the relatively small study area, the mobilization of PTEs during or after any kind of fire events (including controlled burns) are significant because more than a million unrestored legacy mine sites exist worldwide, and many of them are in fire-prone forest regions (Abraham et al., 2018).

Experiments and methods

Sample collection and processing

All plants and soil samples used in this study were collected from Huangshi National Mine Park, Hubei Province, China (30° 13′ N, 114° 55′ E), as shown in Fig. 1. The mine park is located in a historic iron-ore mining area with the largest hard rock afforestation reclamation base in Asia, with an area of about 23.2 km^2. Soil samples were collected from eight sites, including study areas A, B, and C and other areas in the mine park. Five-point sampling method was used

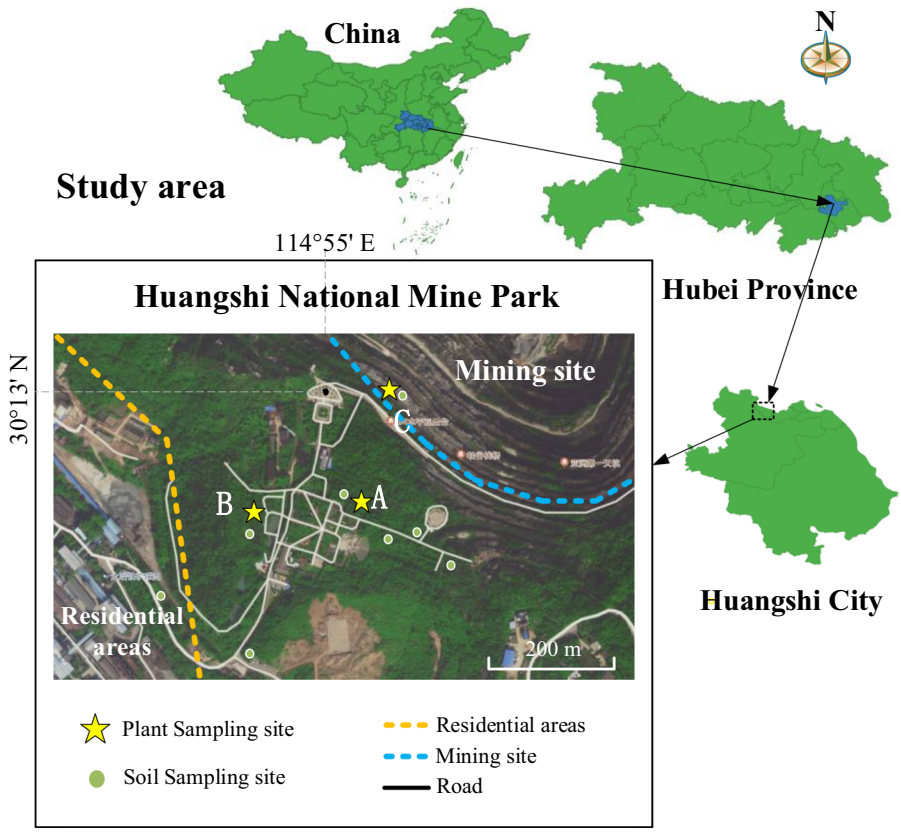

Fig. 1 Location of the study area

to collect the soil at 0–10 cm on the surface soil for each site. The soil collected at five points were mixed and stored in the same polyethylene sample bag and then were transferred to the laboratory. After natural drying in the laboratory, ground and mix thoroughly, and pass through a 100-mesh nylon sieve. The content of PTEs in the soil collected from this mine park is shown in Table 1.

Based on the preliminary survey of the mine park, the vegetation in sites A and B is comprised of arbor, shrubs, and herbaceous plant, and the vegetation in site C is mainly comprised of shrubs and herbaceous plant. Five dominant plants combustibles were selected in the study area: *Camphor leaves* (*CL*), *Camphor dead-branch* (*CB*), *Ramie* (*RA*), *Miscanthus sinensis* (*MS*), and *Dryopteris* (*DR*). Plants combustibles were selected from three sampling sites: A (*CL*, *CB*, *DR*, *MS*, *RA*), B (*CL*, *CB*, *DR*, *MS*, *RA*), and C (*MS*, *RA*). Each sampling site takes 20 m × 20 m as the sample area. 20 samples were collected for each plant in each sampling sites. The ground-fallen leaves and dead branches were collected from *camphor* trees, while the remaining three were collected from the ground part of the plant, sealed and marked after collection, and transferred to the laboratory for storage at 4 °C until processing. In the laboratory, fresh plant samples were processed at 120 °C about half an hour and were dried at 70 °C to keep the water content in the 0–20% range.

To reduce the interference of the shape and size for different plant combustibles, samples were crushed and were passed through 20-mesh and 100-mesh nylon screens, respectively. The samples in the 20–100 mesh range were selected as the experimental fuel for this study. Elemental analysis of five plant combustibles and their moisture content is listed in Table 2.

Combustion experimental apparatus

In this study, the cone calorimeter platform (MOTIS-MCCT, China) was used to conduct combustion experiments of forest combustibles. The cone calorimeter (abbreviated: CONE) was developed by Babrauskas et al. (1992) based on the principle of oxygen depletion, and the construction is shown in the Fig. 2. The advantage is to simulate the burning environment and combustion state of woodland combustible materials more realistically and obtain the characteristic parameters of flammable materials in fire (such as heat release rate, total heat release, and mass loss, and so on). The woodland combustibles were ignited in the combustion chamber while constant thermal radiation was applied to the fuel through the thermal radiation cone, maintaining the combustion of the woodland combustibles until they burned.

The top of the combustion chamber outlet is connected with a stainless steel circular exhaust duct of

Table 1 Average PTEs content of soils in Huangshi National Mine Park and around areas (mg/kg)

Element	Minimum	Maximum	Mean ± SD	Screening value[a]	Control value[a]	GB[b]
As	69.32	307.35	146.20 ± 87.65	60	140	12.30
Be	0.65	3.93	1.70 ± 1.16	29	290	2.08
Co	23.66	136	72.21 ± 41.69	70	350	15.40
Cr	65.70	133.73	96.83 ± 22.99	5.7	78	86
Cd	1.72	7.64	3.515 ± 2.27	65	172	0.17
Cu	417.65	2599.08	1605.27 ± 734.84	18,000	36,000	30.70
Mn	760.12	1314.37	968.09 ± 202.87	–	–	712
Ni	20.62	110.87	68.73 ± 31.59	900	2000	37.30
Pb	30.80	247.45	94.48 ± 78.40	800	2500	26.70
Sb	6.48	24.14	13.60 ± 6.72	180	360	1.65
V	84.68	147.05	110.24 ± 23.04	752	1500	110.20
Zn	388.64	927.14	519.89 ± 213.84	300 (agricultural soil, pH > 7.5); 250 (agricultural soil, 6.5 < pH < 7.5)		83.60

[a]The screening and control values are taken from the reference values recommended in the Chinese Environmental Protection Ministry (CEPM, China) soil Quality standards "GB 36600-2018" and "GB 15618-2018"

[b]GB—Geochemical background values of Hubei Province, China (CNEMC, 1990)

Table 2 Elemental analysis of typical plant combustibles and their moisture content

Plant type	Label	Elemental analysis (wt%)				Moisture content (wt%)
		C	H	N	S	
Camphor leaves	*CL*	46.26	5.400	1.53	0.489	16.36
Camphor dead branches	*CB*	46.09	5.746	0.75	0.219	15.54
Ramie	*RA*	36.45	4.959	2.06	0.420	11.19
Miscanthus sinensis	*MS*	44.50	6.021	1.28	0.201	9.86
Dryopteris	*DR*	36.96	5.410	2.01	0.595	12.33

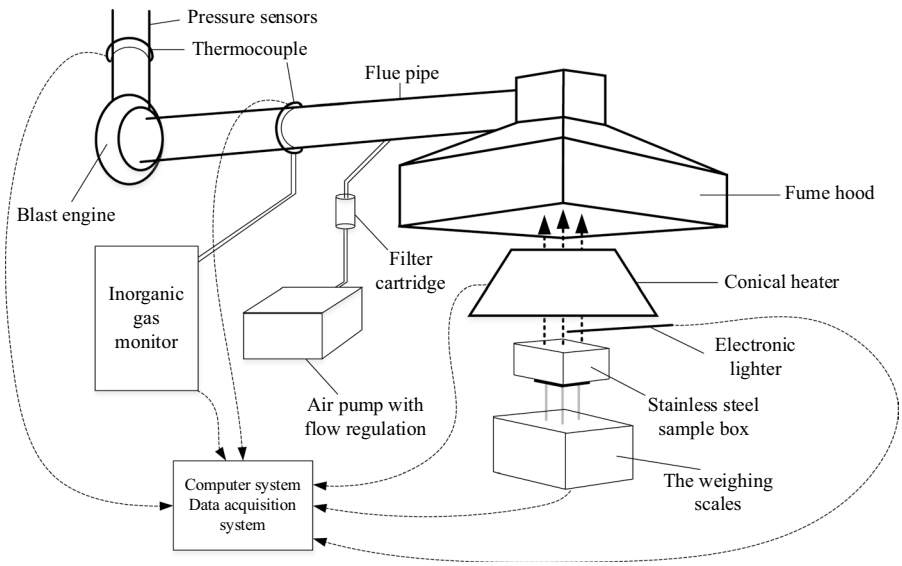

Fig. 2 Schematic illustration of the combustion platform

about 4 m in length and 120 mm in diameter, with pressure sensors, thermocouples, and three sampling ports set up on the side of the exhaust duct in turn. They can measure flue pressure, flue gas temperature, gas flow rate, CO, CO_2, O_2, and collect smoke particles, respectively. Thermocouples in the flue pipe can monitor the temperature change of the flue gas throughout the combustion process. Smoke particles were collected through glass fiber filter cartridges, which were dried at 120 °C and kept at a constant temperature and humidity for 48 h before and after sampling. The combustible samples were placed in a 100 mm × 100 mm × 50 mm stainless steel box with a non-combustible glass wool liner at the bottom so that the distance between the samples and the bottom of the radiation cone was kept at 25 mm.

In this study, thermal radiation temperature and plant type are set as influencing factors. The radiation temperatures were set at 400 °C, 500 °C, 600 °C, 700 °C, and 800 °C to study the effect of radiation temperature on the total content and distribution of PTEs in the smoke particles and residual ashes. Five plant combustibles (*CL*, *CB*, *RA*, *MS*, *DR*) were selected to investigate the differences in the total content and distribution of PTEs in the fire events. The experiment was conducted by heating the radiation cone to the specified temperature, weighing the sample and then igniting it by electronic lighter, and recording the ignition and flame extinguishing time. Based on the literature survey (Dupuy, 1995; Mickler et al., 2002; Sánchez-Pinillos et al., 2021), the forest fuel load was in the range of 0–2 kg/m^2. Based on field sampling calculation, the fuel load range of this study area is 0.5–1.5 kg/m^2, and the average load is close to 1 kg/m^2. Therefore, the fuel load of this experiment was limited to 1.131 kg/m^2, i.e., 10 g was taken for each sample.

Characterization and analysis methods

PTEs content analysis

After each batch experiment, the entire filter cartridge was cut out into small pieces with ceramic scissors, placed in a Teflon beaker, and the residual ash in the box was collected for chemical composition analysis. Each sample was repeatedly burned three times to obtain sufficient products for analysis. All samples were digested by $HCl–HNO_3–H_2O_2/HClO_4$ (CEPM, HJ777/HJ803). The same digestion procedure was operated on the same type and batch of blank glass fiber cartridges to obtain a laboratory blank specimen. After the samples digested, twelve PTEs (As, Be, Co, Cr, Cd, Cu, Mn, Ni, Pb, Sb, V, and Zn) were measured using inductively coupled plasma optical emission spectrometry (ICP-OES, Prodigy 7). The mass concentration of metals in the smoke particles is calculated by Eq. 1.

$$\rho = \frac{(c - c_0) \times V_s \times n}{V_{\text{std}}} \tag{1}$$

where ρ is the mass concentration of metals in smoke particles (μg/m^3), c is the concentration of metals in the specimen (μg/ml), c_0 is the concentration of metals in blank specimens (μg/ml). V_s is fixed volume after digestion (ml), and n is the ratio of the area of the sampling filter membrane to the area taken during digestion for filter cartridges $n = 1$. V_{std} is the sampling volume of dry flue gas at standard condition (m^3).

BCR sequential extraction procedure

BCR Sequential extraction procedure is a three-step sequential extraction procedure for sediment analysis, which was proposed by the European Community Bureau of Reference (BCR). PTEs speciation of residual ashes was analyzed according to the procedures of Rauret et al. (1999). The adopted process separated PTEs into four operationally defined fractions including acid-soluble (extractable), reducible, oxidizable, and residual fraction (Dundar et al., 2012; Fernandez et al., 2004). The detailed process is shown in Table S4.

Risk evaluation method

The combustible load in this study was determined by literature research and field surveys in the mine park. It was used to estimate the risk of PTEs contamination in a forest fire in the woodland of the mine park. The risk evaluation calculation of PTEs mainly refers to geochemical background value of soil from Hubei province (CNEMC, 1990) and the control values recommended in the Chinese Environmental Protection Ministry (CEPM, China) soil Quality standards "GB 36600-2018" and "GB 15618-2018." The values are shown in Table 1.

Geo-accumulation index

The method was proposed by Muller (1969) and was widely used in Europe for the study of PTEs. It can assess the environmental contamination of PTEs by comparing differences between current and pre-industrial PTEs concentrations. The calculation formula is shown in Eq. 2:

$$I_{\text{geo}} = \log_2 \frac{C_i}{1.5 \times GB_i} \tag{2}$$

where C_i is the measured concentration of PTEs i found in the smoke particles and ash (mg/kg), and GB_i is the geochemical background value of the PTE i (mg/kg), which is taken from Hubei province soil background values (CNEMC, 1990). 1.5 is the coefficient considering the variation of background values caused by rock differences in different places. The I_{geo} consists of seven grades (Table S5).

Comprehensive pollution evaluation of PTEs

Residual ashes from biomass combustion can be deposited on the surface of soil. To quantify the PTEs contamination risk of residual ashes after fire event, the single pollution index (P_i) and the Nemerow pollution index (NPI) were applied in this study (Kowalska et al., 2018; Ma et al., 2018). The formula is as follows:

$$P_i = \frac{C_i}{S_i} \tag{3}$$

$$\mathrm{NPI} = \sqrt{\frac{P_{i\max}^2 + \left(\frac{1}{n}\sum P_i\right)^2}{2}} \quad (4)$$

where P_i is the contamination index of single PTE i, P is the evaluation index of residual ashes pollution. S_i is the reference value (mg/kg) for pollutant i, calculated using the soil as mentioned above pollution risk control values, and n is the number of PTEs involved in the evaluation. The NPI consists of five grades (Table S6).

Quality assurance and control

A parallel double sample test was carried out for every ten samples. Two blank specimens (including cartridge blank and reagent blank) were measured for each batch of samples. Standard curves were established as required before determining each batch of samples. Calibration standard curves for all PTEs had strong linear responses ($R^2 = 0.9991$–0.9997, Table S7).

Data analysis

Spearman rank correlation coefficients were used to get the relationships among the physicochemical properties and combustion characteristics of fuel and the corresponding concentrations of the PTEs in the smoke/ash, include relationship between the PTEs themselves.

Results and discussion

Heat release characteristics of combustibles

As shown in Table 3, for the same plant *CL*, with the temperature increasing, the time to ignition (TTI) became shorter, the time to flame extinction (TFE) gradually advanced, and the total heat release (THR) increased gradually. The peak of heat release rate (pkHRR) also increased gradually. It was shown that the higher the temperature of thermal radiation was, the faster and more complete the combustible fuel burnt, the faster the flame propagated. Meanwhile, the carbon formation rate (CFR) decreased plant with the increase of radiation temperature, indicating that the higher the fire temperature is, the more completely it burns, and the less residual ash there is.

For different types of plant combustibles, when the radiation temperature was 600 °C, the TTI of different plant was ranked as $\mathrm{TTI}_{MS} < \mathrm{TTI}_{CL} < \mathrm{TTI}_{CB} < \mathrm{TTI}_{RA} < \mathrm{TTI}_{DR}$. The TFE was ranked as $\mathrm{TFE}_{MS} < \mathrm{TFE}_{DR} < \mathrm{TFE}_{CL} < \mathrm{TFE}_{CB} < \mathrm{TFE}_{RA}$, indicating that *MS* has the worst fire resistance and is most likely to ignite for the five combustibles, followed by *CL*. It was also found that *DR*′ TTI was the slowest, but the TFE for *DR* was second only to *MS*, indicating that the combustible fuel would be ignited and burned faster. In addition, the THR and pkHRR were ranked as $CB > RA > MS > CL > DR$. This shows that although *CB* burnt for a long time, the heat released once ignited is higher than the other four combustible fuels. Hence, there is a greater fire hazard.

Table 3 Parameters and characteristics of combustion experiments

	T (°C)	Load capacity (kg/m^2)	TTI (s)	TFE (s)	Flue gas average temperature (°C)	THR (MJ/m^2)	pkHRR (Kw/m^2)	CFR (%)
CL	400	1.14	57	182	39.57 ± 3.14	4.83	82.5	15.71
	500	1.13	41	163	42.56 ± 2.90	6.16	81.93	15.36
	600	1.13	12	135	48.25 ± 3.16	6.82	92.5	14.32
	700	1.13	8	112	53.54 ± 3.78	7.01	114.22	12.80
	800	1.15	4	109	62.39 ± 4.23	7.93	133.57	11.04
CB	600	1.14	22	146	47.17 ± 3.40	10.47	146.43	10.64
RA	600	1.14	28	166	49.46 ± 4.29	9.24	118.79	18.75
MS	600	1.16	10	114	50.14 ± 4.33	8.16	117.84	13.91
DR	600	1.14	30	119	50.13 ± 3.98	5.93	93.71	12.11

PTEs in smoke particles

As shown in Fig. 3a, the mass concentration of PTEs generated by combustion in the five plants (*CL*, *CB*, *RA*, *MS,* and *DR*) was significantly different. For As, the maximum value of smoke particles of sample *CB* was 67.09 μg/m^3, while element of sample *DR* was not detected due to the detection limit. For Cr, the highest and lowest concentrations were 75.42 μg/m^3 and 12.39 μg/m^3, respectively, for *CL*. In particular, the highest concentrations of Cu, Mn, Pb, Sb, and V were 72.78 μg/m^3 (*CB*), 115.48 μg/m^3 (*RA*), 113.51 μg/m^3 (*CB*), 113.52 μg/m^3 (*CL*), and 125.89 μg/m^3 (*CL*), respectively. The lowest values were 12.06 μg/m^3 (*MS*), 10.18 μg/m^3 (*CL*), 14.64 μg/m^3 (*RA*), 6.56 μg/m^3 (*CL*), and 58.05 μg/m^3 (*MS*), with a 2–17 time difference in mass concentration. In general, for five plant combustible, the smoke particles after *CB* combustion had a high concentration of PTEs and a high hazard potential. Hence, more attention should be paid on it.

The content of PTEs in the smoke particles generated from *Camphor leaves* (*CL*) was also different at different radiation temperatures. Most of PTEs (such as Cr, Cu, Mn, Ni, Pb, Sb, and Zn) had higher mass concentrations measured at 400 °C. However, with the increase of temperature, the concentration of PTEs decreased at different degrees. The mass concentrations of some PTEs increased first and then fell with the rise of temperature (such as As, V element).

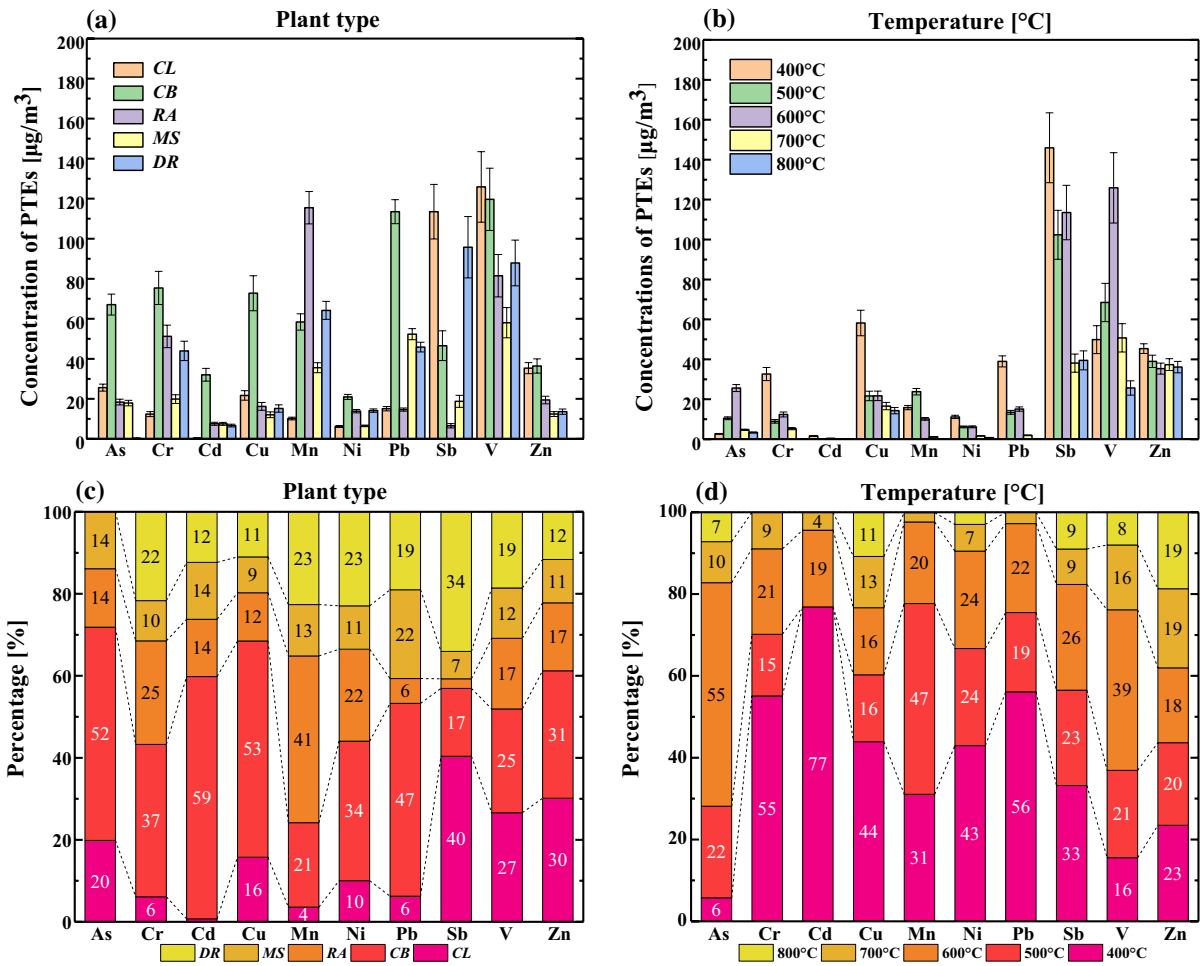

Fig. 3 Concentrations of PTEs in smoke particles (**a** plant types, **b** temperatures) and their percentage concentrations (**c** plant types, **d** temperatures)

The low content of Be and Co in the particulate matter is not shown in Fig. 3.

PTEs in residual ashes

Phase analysis of residual ashes by XRD

Biomass ash is a non-homogeneous material consisted mainly of granular carbon, oxides of basic cations and hydroxides, silicon oxide, etc. (Abraham et al., 2017; Khanna et al., 1994). XRD analysis were performed on residual ashes samples at radiation temperatures of 400 °C, 600 °C, and 800 °C, and the results are shown below.

As shown in Fig. 4, from the X-ray diffraction pattern, it was clear that the main phase in the residual ashes after combustion at 400 °C and 600 °C was $CaCO_3$. In addition, SiO_2 and CaO phases were found at 400 °C; However, CaO phases were not found at 600 °C, probably because $CaCO_3$ was formed by the reaction of CaO with CO_2 at this time, which also corresponded to the increase in $CaCO_3$ peak intensity. When the temperature was 800 °C, the characteristic peaks of $CaCO_3$ and CaO were mainly present in the diffraction pattern, and the highest peak intensity changes to CaO at this time. Because $CaCO_3$ decomposes probably to CaO and CO_2 at 800 °C, this leads to the increase of CaO content in the residual ashes at this time, and the results were consistent with the study of Xiaopin et al. (2010) (Fig. 4)

PTEs content analysis

Plant type can affect the content and distribution of PTEs in residual ashes (Campos et al., 2016). According to section 'Heat release characteristics of combustibles,' the residual ashes content accounted for 10.64–18.75% of the total amount of the samples after the combustibles of the five plants were burned. Different plant types have various enrichment capacities for PTEs, leading to separate release of PTEs after combustion. Figure 5 shows that Be, Co, Cr, Cu, Mn, Ni, Pb, V, and Zn accounted for a large proportion of the residual ashes generated by the combustion of sample *CL*. The contents of As, Pb and Zn in residual ashes of *CB* were higher than those of other combustibles. The content of Cd in *RA′* residual ashes was higher than that of other combustibles. In addition, the content of As, Cd, and Sb in residual ashes of *MS* was higher than the others. In particular, the element Be was only detected in the residual ashes of *CB* and *DR*.

The radiation temperature can affect PTEs ratio. As shown in Fig. 5b, the contents of elements Co, Cr, Cu, Mn, Ni, Pb, Sb, V, and Zn in the residual ashes of *CL* increased to various degrees with the increase of temperature. In contrast, the content of Cd was relatively stable. Jagustyn et al. (2017) pointed out that Cd began to evaporate at about 830 °C. This may have contributed to the relatively stable Cd content in residual ashes (the maximum temperature in this study was 800 °C). Element of As decreased with the increase of temperature. It may be due to the relative intense volatility of As element (Jagustyn et al., 2017), which volatilized from plant residual ashes in this temperature range. The variation trend of content percentage of As in the residual ashes was corresponding to the ratio of As in the particle. However, As and some of PTEs ratio significantly increased at 800 °C. The PTEs in the residual ash may react with SiO_2 and Al_2O_3 in the residual ashes at this time, leading to the decrease of PTEs volatility. Moreover, CaO of residual ashes may adsorb some PTEs evaporated at high temperature, which makes PTEs concentrate in residual ashes (Punjak et al., 1989; Yu et al., 2016). The aforementioned XRD phase analysis results also showed that the characteristic peak of CaO in residual ashes at 800 °C was stronger. In general, residual ashes composition may play a role in the further migration of PTEs after the fire. Both fire temperature and plant type caused a difference in a PTEs release.

The fractional distribution of Cr and As in residual ashes

The actual bioavailability and pollution potential of PTEs in residual ashes mainly depend on the speciation distribution of PTEs (Maiz et al., 1997; Sungur et al., 2014). The speciation of PTEs is the basis of their bioavailability. According to the BCR continuous extraction method classification, soluble acid (F1) and reducible acid (F2) are easy to be leached in weak acid or neutral environments and absorbed directly by plant due to strong migration. Oxidative (F3) PTEs do not quickly release in an alkaline environment, but easily transform into F1 and F2 in an acidic environment, which has potential ecological risks. The

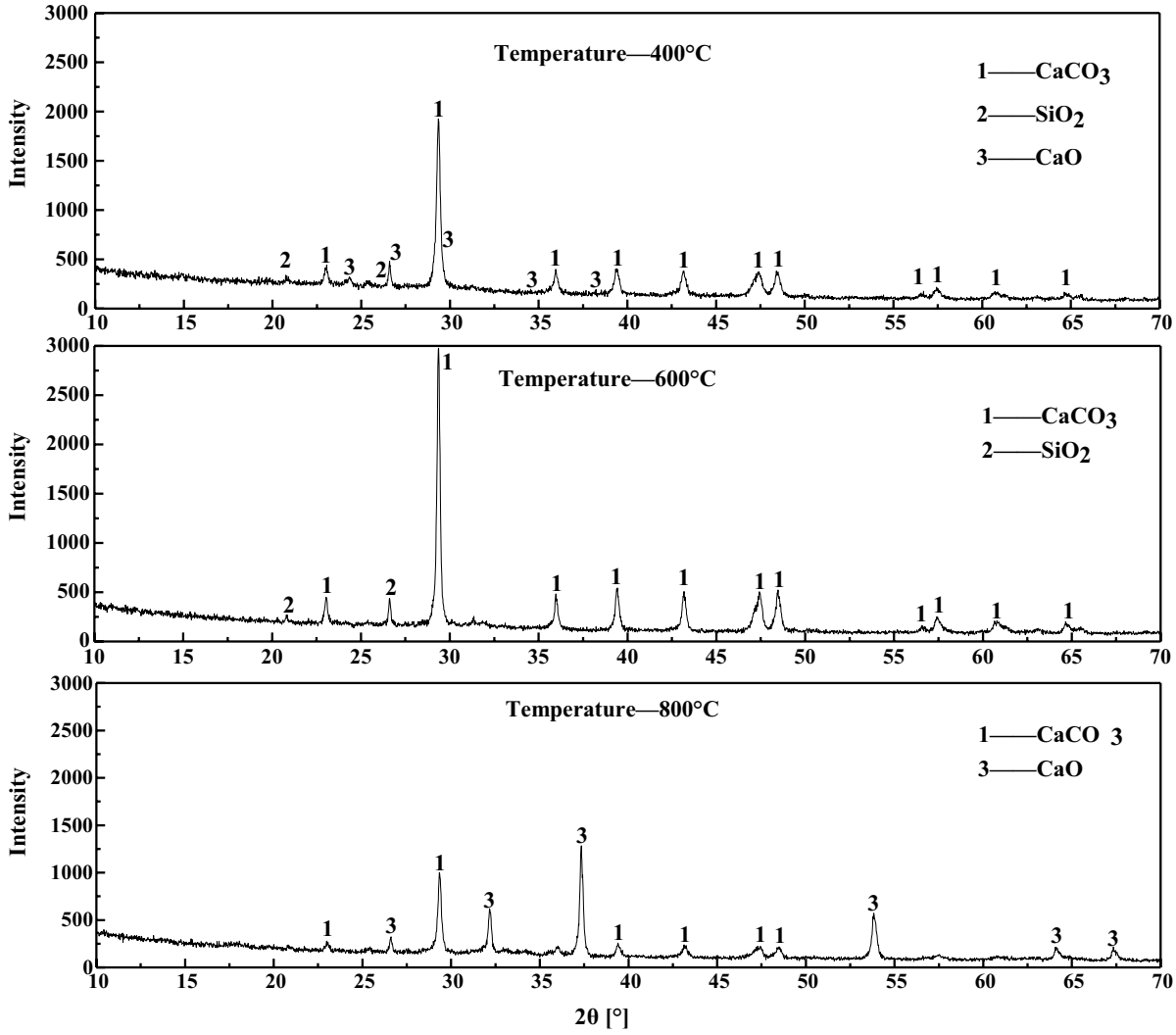

Fig. 4 XRD physical phase analysis of residual ashes

residual state (F4) is the most stable. Understanding the speciation distribution of PTEs after biomass combustion can effectively evaluate its potential pollution capacity.

Figure 6 shows the differences in the forms of Cr and As in the combustion residual ashes of different plant types. The proportions of Cr in the residual state (F4) of *CL*, *RA*, and *MS* were 81%, 39%, and 77%, respectively. The residual state of Cr was higher than other states, indicating that it mainly existed in a stable form in the residual ashes and then in an oxidizable state. However, the available state of F1 + F2 accounted for 25% of Cr in *RA′* residual ashes, suggesting some degree of mobility. The available states of As accounted for 57%, 69%, and 50% in the residual ashes for three plants, respectively, showing high migration potential and bioavailability. The available proportions of Cr and As in *RA′* residual ashes were higher than in the others' plant, indicating that plant type may affect the migration and bioavailability of PTEs in the environment after direct combustion.

The speciation analysis of As in residual ashes from different temperatures showed that the available state (F1 + F2) gradually decreased from 74% (400 °C) to 41% (800 °C) with the increase of

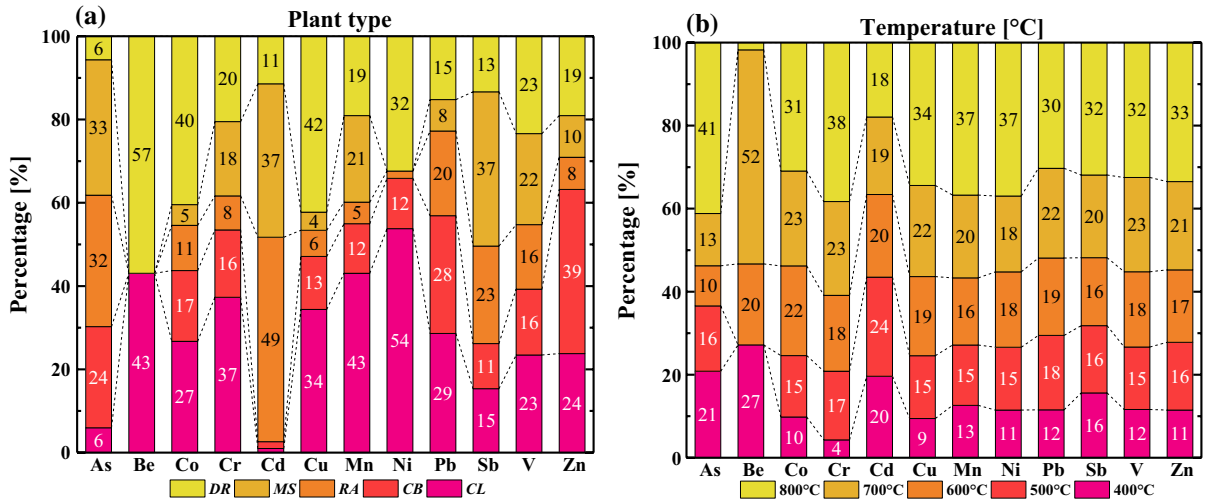

Fig. 5 Content percentage of PTEs in residual ashes after combustion (**a** different plant types, **b** different radiation temperatures)

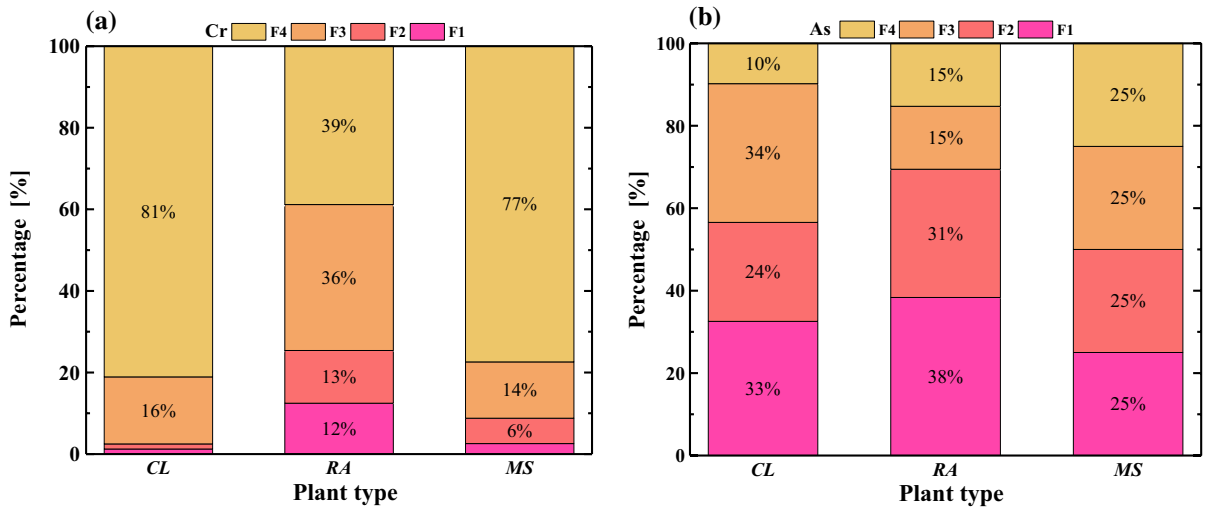

Fig. 6 Speciation distribution percentages of Cr and As in combustion residual ashes of different plant types

temperature, indicating that the rise of thermal radiation significantly reduced the migration potential and bioavailability of As. In this study, most of As existed in the oxidizable state in residual ashes. Since the proportion of available states of As was high, and it was easy to migrate with ash, its potential environment pollution and its impact on downstream water should be further studied and determined. The difference was that most of the Cr in residual ashes in this study existed in the oxidizable state and residual state, and its effective state F1 + F2 ranged from 2 to 9%, showing relatively low mobility and bioavailability. This indicates that bioavailability of Cr was less affected by radiation temperature. However, it was known that Cr content in residual ashes increased significantly with the increase of radiation temperature and exceeded the soil control value (CEPM, GB 36600-2018). Therefore, migration potential and human health risk of Cr cannot be ignored when its release exceeded the limit value (Fig. 7).

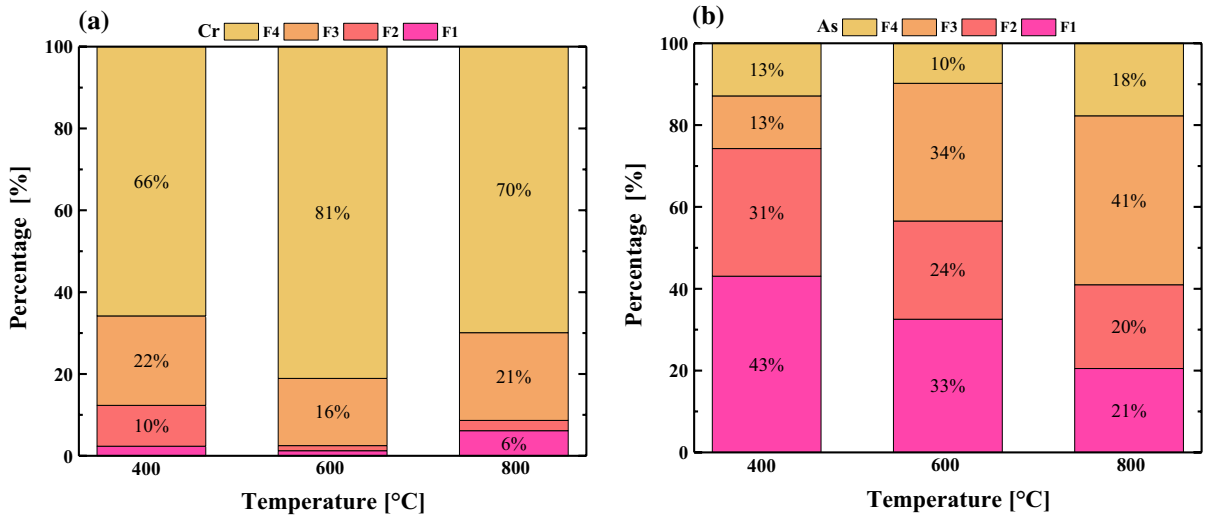

Fig. 7 Speciation distribution percentage of Cr and As in residual ashes combustion of sample *CL* at different radiation temperatures

Relationship of PTEs in smoke particles and residual ashes with physicochemical properties

Previous studies focused on the role of pH, Electrical conductivity (EC) and organic matter (OM) in the retention and mobilization of PTEs in the environment (Abraham et al., 2018; Campos et al., 2016). In this study, the relationship between PTEs content in smoke particles (Table S8) and residual ashes (Table S9) with physicochemical characters such as TTI, TFE, THR, CFR, and CHNS elements were assessed with the Spearman rank correlation method. The "r=0.80–1.0" and "r=0.6–0.79" mean very strong and strong correlations, respectively.

The physicochemical properties of plant combustibles and PTEs in the smoke particles displayed little strong correlations (Table S8), except moisture content (wt%) showed a strong negative correlation with Mn (r=−0.803), and C element displayed strong negative correlation with Mn (r=−0.895). The TTI, TFE, and CFR did not show significant correlation with any of the PTEs in the smoke particles. Mean temperature of gas showed a moderate correlation with Cu (r=−0.783) and Sb (r=-0.667).

When the moisture content was considered, it showed a strong correlation with Cd (r=−0.895) and Ni (r=0.895),and a moderate correlation with Mn (r=0.785) and Pb (r=0.694) in residual ash. This indicated that the initial biomass moisture content affected the content of Cd, Ni, Mn and Pb in ash, consistent with the research results of Hu et al. (2014) (moisture content in the range of 0–25%). When heat release characteristics of plant combustibles were considered, the THR and CFR did not show a significant correlation with any of the PTEs in the residual ashes, except THR with As (r=0.667) and CFR with Zn (r=−0.750). The results showed that the content of As in ash was affected by the THR of plant. Although the correlation is not strong, the THR represents the total heat release of fuel, which is closely related to the fire severity. When we considered elemental analysis of plant combustibles, C element showed a strong correlation with Cd (r=−0.895), Mn (r=0.858), and Ni (r=0.822). The element of H and N did not show any significant correlation with any of the PTEs in the residual ashes, except S with As (r=−0.822), Co (r=0.822), and Cu (r=0.840), and a moderate correlation with Be (r=0.686). The results showed that the presence of As, Cu, and Co in ash was affected by the content of sulfur in biomass. Miller et al. (2003) also found that sulfur had an impact on the content of As and Cu in ash, but the performance of As was inconsistent with that in this paper, which may be caused by the different content of sulfur in the combustion process.

The correlations between PTEs (themselves) in residual ashes displayed a number of very strong and strong correlations. For example, Co displayed strong positive correlation with Cu (r=0.967) and a moderate correlation with Cr (r=0.733), Ni (r=0.717) and

V ($r=0.717$). Cr displayed strong positive correlation with Mn ($r=0.883$), Ni ($r=0.833$), and V ($r=0.933$) and a moderate correlation with Cd ($r=-0.700$), Cu ($r=0.783$), Pb ($r=0.683$), and Zn ($r=0.717$). Abraham et al. (2018) also found correlations between Cr and Mn, Zn, and Ni in field controlled combustion experiments. Cd showed strong negative correlation with Mn ($r=-0.883$) and Ni ($r=-0.917$) and a moderate correlation with Cu ($r=-0.683$), Pb ($r=-0.783$) and Zn ($r=-0.717$). The strong and very strong correlations between metals highlighted their common origin.

Environment risk evaluation

Geo-Accumulation Index

Figure 8 shows the range of geo-accumulation index of PTEs in residual ashes generated by different plant and different radiation temperatures. From Fig. 8a, the geo-accumulation index values of As, Co, and Ni changed significantly. The pollution levels ranged from no pollution to strong pollution. It indicated that the pollution level of PTEs in residual ashes may be affected considerably by plant types. In addition, the 75th percentile of I_{geo} values of Cd, Cu, Pb, Sb, and Zn were all greater than zero, indicating that these elements may cause environmental pollution. According to the median value of I_{geo} value, the pollution degree of these PTEs under different plant types was roughly ranked as Pb > As/Zn/Cu > Cd/Sb > Co.

Figure 8b shows that the I_{geo} values of As, Co, Cr, Mn, and Ni varied greatly from no pollution to moderate pollution, or even extremely polluted (Ni). It suggests that the temperature affects the pollution potential of the above PTEs. The I_{geo} of PTEs in the burning residual ashes of *CL* was almost greater than zero (except Be and V elements), indicating that PTEs in residual ashes may cause light to moderate or above degree of pollution to the environment. Based on the median value of I_{geo}, the pollution degree of these PTEs under different radiation temperatures was roughly as Mn > Co > Ni/Pb > Zn > Cd/Cu/Sb > Cr > As.

The range of PTEs' I_{geo} values in smoke particles generated under different plant combustion and radiation temperatures is shown in Fig. 9. Based on the median line of I_{geo} value, PTEs pollution in smoke particles generally presented a mild-to-moderate pollution level, and the I_{geo} value was between 0 and 1. However, at different radiation temperatures, the value of *MS'* I_{geo} varied greatly, ranging from no pollution to moderate pollution.

Comprehensive evaluation of PTEs pollution

The evaluation results of NPI method are shown in Table 4. With the increase of radiation temperature, the NPI values gradually increased, indicating that the overall pollution level of residual ashes PTEs rose from low pollution to high pollution level. In terms of residual ashes content of different plant, the

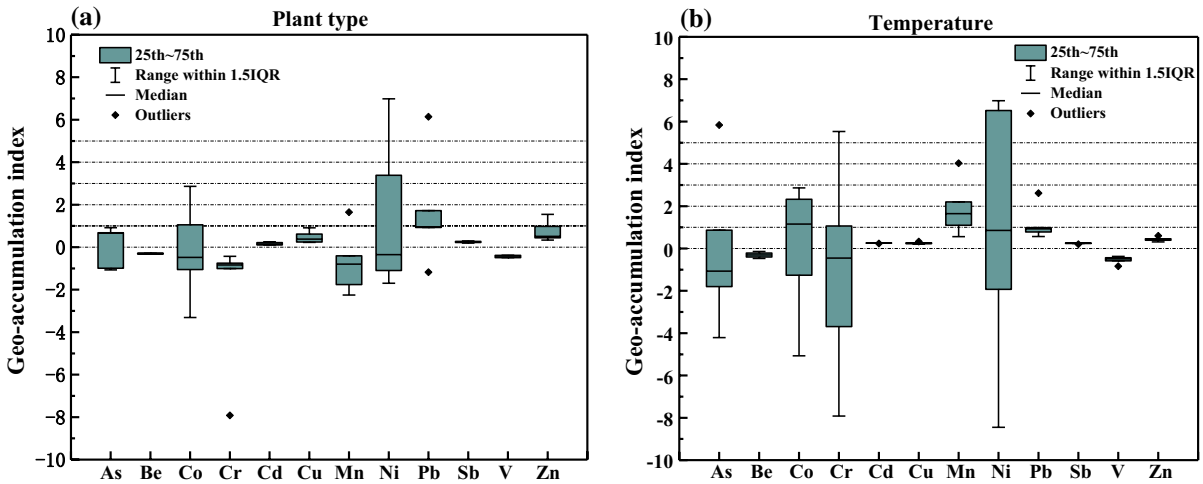

Fig. 8 Box plot of PTEs I_{geo} in biomass residual ashes (**a** plant type; **b** radiation temperature)

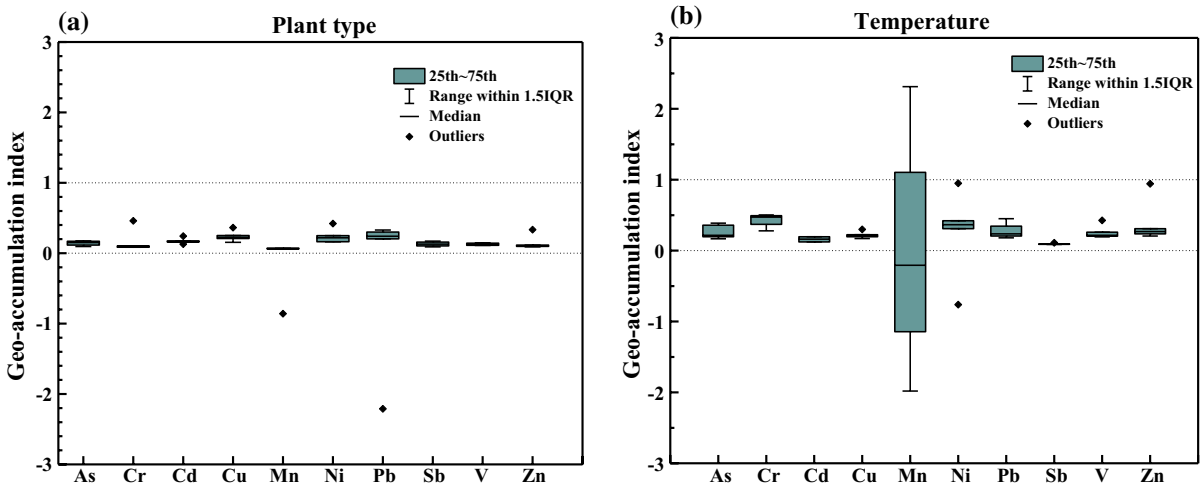

Fig. 9 Box plot of PTEs I_{geo} in smoke particles (**a** plant type; **b** radiation temperature)

Table 4 Pollution level of PTEs in residual ashes

Types	T (°C)	Single factor pollution index P_i										*NPI*	Level
		As	Co	Cr	Cd	Cu	Ni	Pb	Sb	V	Zn		
CL	400	0.15	0.04	0.36	0.02	0.01	0.02	0.02	0.10	0.02	1.33	0.95	Low
	500	0.11	0.06	1.37	0.03	0.02	0.03	0.03	0.10	0.02	1.89	1.35	Moderate
	600	0.07	0.08	1.52	0.02	0.02	0.03	0.03	0.10	0.03	2.02	1.45	Moderate
	700	0.09	0.09	1.87	0.02	0.02	0.03	0.04	0.13	0.03	2.46	1.76	Moderate
	800	0.29	0.12	3.17	0.02	0.04	0.06	0.05	0.20	0.05	3.87	2.78	High
CB	600	0.28	0.05	0.66	0.04	0.01	0.01	0.03	0.07	0.02	3.35	2.38	High
RA	600	0.36	0.03	0.33	1.15	0.00	0.00	0.02	0.16	0.02	0.66	0.83	Low
MS	600	0.38	0.02	0.72	0.86	0.00	0.00	0.01	0.25	0.02	0.85	0.64	Clean
DR	600	0.07	0.13	0.83	0.27	0.03	0.02	0.02	0.09	0.03	1.62	1.16	Moderate

overall pollution level of PTEs in the residual ashes of *CB* was the highest, and the NPI value of the pollution index was the highest. Both *CL* and *DR* showed moderate pollution. The *RA′* residual ashes content showed a low pollution level, and the pollution index NPI value was slightly higher than 0.7. The NPI value of *MS* is lower than 0.7, indicating no pollution.

From the perspective of single factor pollution index P_i, the P_i values of Cr and Zn were on the high side as a whole, with the highest value of 3.17 for NPI (Cr) and 3.87 for NPI (Zn). The results indicated that Cr and Zn were the main pollution elements in the residual ashes content in this study. In addition, the single factor index values of Cd in residual ashes of *MS* and *RA* were up to 1.15 and 0.86, respectively, and the other elements were lower than 0.7, indicating that Cd was one of the main pollution elements in *RA* and *MS*. In general, $NPI_{CL,\ 800} > NPI_{CB} > NPI_{CL,\ 700} > NPI_{CL,\ 600} > NPI_{CL,\ 500} > NPI_{DR} > NPI_{CL,\ 400} > NPI_{RA}$.

Conclusion

In this paper, the total content and fractional distribution of PTEs in smoke particles and residual ashes from mine-park-biomass combustion were studied. The effects of radiation temperatures and plant types on the release of PTEs were explored, and the consequential potential fire environmental risk was evaluated. The results showed that the sample *CB* had a high potential for PTEs release.

Low temperature (400 °C) may benefit the enrichment of Cr, Cu, Mn, Ni, Pb, and Sb in smoke particles. In comparison, high temperatures (800 °C) may benefit the enrichment of some PTEs in residual ashes. The fractional analysis of As and Cr elements showed that As had a higher proportion of available states in residual ashes, while Cr mainly existed in oxidizable and residual states, and its migration and bioavailability were much lower than As. The risk assessment results showed that PTEs in smoke particles and residual ashes might cause light to moderate or above degree of pollution to the environment. The overall pollution level of PTEs in residual ashes of *CB* was the highest, and Cr and Zn were the main pollution elements in residual ashes. In general, the biomass combustion in the woodland of mining areas leads to the release of PTEs and lead to environment pollution.

The cone calorimeter provides a convenient method for forest fuel combustion and PTEs occurrence. It provides a repeatable and low-cost source of raw data for modeling the migration and transformation of pollutants after combustion. This study has important practical significance for understanding the environment risk of mining areas and surrounding forest areas that can be reclaimed as agricultural land, forestry land, and ecological park. It clarifies the practical significance of strengthening fire monitoring and control in mining forestlands and preventing the spread and migration of PTEs through forest fire from the source.

Acknowledgements The authors are grateful for the financial support of National Natural Science Foundation of China (51504174 and 51876148) and the technical support from the Analytical and Testing Center of Wuhan University of Technology.

Author contributions All authors contributed to the study conception and design. Material preparation, data collection, and analysis were performed by [XY], [BZ], [ZT] and [CL]. The combustion experiments were instructed by [KL]. The manuscript was written and finalized by [YL] and all authors commented on the manuscript. All authors read and approved the final manuscript.

Funding This work was supported by National Natural Science Foundation of China (Grant numbers [51504174] and [51876148]).

Data availability All data generated or analyzed during this study are included in this published article (and supplementary information files).

Code availability Not applicable.

Declarations

Conflict of interest The authors declare that they have no conflict of interest.

Ethical approval Not applicable.

Consent to participate Not applicable.

Consent for publication All authors have given consent to the publication of this article.

References

Abraham, J., Dowling, K., & Florentine, S. (2017). The unquantified risk of post-fire metal concentration in soil: A review. *Water Air & Soil Pollution, 228*(5), 175. https://doi.org/10.1007/s11270-017-3338-0

Abraham, J., Dowling, K., & Florentine, S. (2018). Controlled burn and immediate mobilization of potentially toxic elements in soil, from a legacy mine site in Central Victoria, Australia. *Science of the Total Environment, 616–617*, 1022–1034. https://doi.org/10.1016/j.scitotenv.2017.10.216

Babrauskas, V., Twilley, W. H., Janssens, M., & Yusa, S. (1992). Cone calorimeter for controlled-atmosphere studies. *Fire and Materials, 16*(1), 37–43. https://doi.org/10.1002/fam.810160106

Barbero, R., Abatzoglou, J. T., Larkin, N. K., Kolden, C. A., & Stocks, B. (2015). Climate change presents increased potential for very large fires in the contiguous United States. *International Journal of Wildland Fire, 24*(7), 892–899. https://doi.org/10.1071/WF15083

Beda, P. X. Ã. (2010). Spatial distribution of heavy metals released from ashes after a wildfire. *Journal of Environmental Engineering and Landscape Management, 18*(1), 13–22. https://doi.org/10.3846/jeelm.2010.02

Burges, A., Alkorta, I., Epelde, L., & Garbisu, C. (2018). From phytoremediation of soil contaminants to phytomanagement of ecosystem services in metal contaminated sites. *International Journal of Phytoremediation, 20*(4), 384–397. https://doi.org/10.1080/15226514.2017.1365340

Campos, I., Abrantes, N., Keizer, J. J., Vale, C., & Pereira, P. (2016). Major and trace elements in soils and ashes of eucalypt and pine forest plantations in Portugal following a wildfire. *Science of the Total Environment, 572*, 1363–1376. https://doi.org/10.1016/j.scitotenv.2016.01.190

Campos, I., Vale, C., Abrantes, N., Keizer, J. J., & Pereira, P. (2015). Effects of wildfire on mercury mobilisation in eucalypt and pine forests. *CATENA, 131*, 149–159. https://doi.org/10.1016/j.catena.2015.02.024

CEPM, & BLR. (2014, 2019-12-28). *Survey report on soil pollution in China*. http://www.gov.c-n/xinwen/2014-04/17/content_2661765.htm

Chen, C. J., Chiou, H. Y., Chiang, M. H., Lin, L. J., & Tai, T. Y. (1996). Dose–response relationship between ischemic

heart disease mortality and long-term arsenic exposure. *Arteriosclerosis, Thrombosis, and Vascular Biology, 16*(4), 504. https://doi.org/10.1161/01.ATV.16.4.504

CNEMC. (1990). *The soil background value in China*. China Environmental Science Press.

Costa, M. R., Calvão, A. R., & Aranha, J. (2014). Linking wildfire effects on soil and water chemistry of the Maro River watershed, Portugal, and biomass changes detected from Landsat imagery. *Applied Geochemistry, 44*, 93–102. https://doi.org/10.1016/j.apgeochem.2013.09.009

DeBano, L. F. (2000). The role of fire and soil heating on water repellency in wildland environments: A review. *Journal of Hydrology, 231*(NO.Special SI), 195–206. https://doi.org/10.1016/S0022-1694(00)00194-3

Dudka, S., & Adriano, D. C. (1997). Environmental impacts of metal ore mining and processing: A review. *Journal of Environmental Quality, 26*(3), 590–602. https://doi.org/10.2134/jeq1997.00472425002600030003x

Duffus, J. H. (2001). "Heavy Metals"—A meaningless term. *Chemistry International-Newsmagazine for IUPAC, 23*(6), 163–167. https://doi.org/10.1351/pac200274050793

Dundar, M. S., Altundag, H., Eyupoglu, V., Keskin, S. C., & Tutunoglu, C. (2012). Determination of heavy metals in lower Sakarya river sediments using a BCR-sequential extraction procedure. *Environmental Monitoring & Assessment, 184*(1), 33–41. https://doi.org/10.1007/s10661-011-1944-7

Dupuy, J. L. (1995). Slope and fuel load effects on fire behavior: Laboratory experiments in pine needles fuel beds. *International Journal of Wildland Fire, 5*(3), 153–164. https://doi.org/10.1071/WF9950153

Ebel, B. A., & Moody, J. A. (2017). Synthesis of soil-hydraulic properties and infiltration time-scales in wildfire-affected soils. *Hydrological Processes, 31*(2), 324–340. https://doi.org/10.1002/hyp.10998

Fernandez, E., Jimenez, R., Lallena, A. M., & Aguilar, J. (2004). Evaluation of the BCR sequential extraction procedure applied for two unpolluted Spanish soils. *Environmental Pollution, 131*(3), 355–364. https://doi.org/10.1016/j.envpol.2004.03.013

Fraser, R. H., & Li, Z. (2002). Estimating fire-related parameters in boreal forest using spot vegetation. *Remote Sensing of Environment, 82*(1), 95–110. https://doi.org/10.1016/S0034-4257(02)00027-5

Grigal, D. F. (2003). Mercury sequestration in forests and peatlands: A review. *Journal of Environmental Quality, 32*(2), 393–405. https://doi.org/10.2134/jeq2003.0393

Gutiérrez, M., Mickus, K., & Camacho, L. M. (2016). Abandoned PbZn mining wastes and their mobility as proxy to toxicity: A review. *Science of the Total Environment, 565*, 392–400. https://doi.org/10.1016/j.scitotenv.2016.04.143

Hodson, M. E. (2004). Heavy metals—Geochemical bogey men? *Environmental Pollution, 129*(3), 341–343. https://doi.org/10.1016/j.envpol.2003.11.003

Hu, R., Liu, J., & Zhai, M. (2011). *Mineral resources science and technology in China: A roadmap to 2050*. Springer Science & Business Media.

Hu, Y., Wang, J., Deng, K., & Ren, J. (2014). Characterization on heavy metals transferring into flue gas during sewage sludge combustion. *Energy Procedia, 61*, 2867–2870. https://doi.org/10.1016/j.egypro.2014.12.325

Jagustyn, B., Kmie, M., Dowski, S., & Sajdak, M. (2017). The content and emission factors of heavy metals in biomass used for energy purposes in the context of the requirements of international standards. *Journal of the Energy Institute, 90*(5), 704–714. https://doi.org/10.1016/j.joei.2016.07.007

Jakubus, M., Kaczmarek, Z., Michalik, J., & Grzelak, M. (2010). The effect of different tree plantings and soil preparation methods on contents of selected heavy metals in post-fire soils. *Fresenius Environmental Bulletin, 19*(2a), 312–317.

Kelly, E. N., Schindler, D. W., St Louis, V. L., Donald, D. B., & Vlaclicka, K. E. (2006). Forest fire increases mercury accumulation by fishes via food web restructuring and increased mercury inputs. *Proceedings of the National Academy of Sciences of the United States of America, 103*(51), 19380–19385. https://doi.org/10.1073/pnas.0609798104

Khanna, P. K., Raison, R. J., & Falkiner, R. A. (1994). Chemical properties of ash derived from Eucalyptus litter and its effects on forest soils. *Forest Ecology & Management, 66*(1–3), 107–125. https://doi.org/10.1016/0378-1127(94)90151-1

Kowalska, J. B., Mazurek, R., Gąsiorek, M., & Zaleski, T. (2018). Pollution indices as useful tools for the comprehensive evaluation of the degree of soil contamination—A review. *Environmental Geochemistry and Health, 40*(6), 2395–2420. https://doi.org/10.1007/s10653-018-0106-z

Liu, H., Probst, A., & Liao, B. (2005). Metal contamination of soils and crops affected by the Chenzhou lead/zinc mine spill (Hunan, China). *Science of the Total Environment, 339*(1–3), 153–166. https://doi.org/10.1016/j.scitotenv.2004.07.030

Ma, W., Tai, L., Qiao, Z., Zhong, L., Wang, Z., Fu, K., & Chen, G. (2018). Contamination source apportionment and health risk assessment of heavy metals in soil around municipal solid waste incinerator: A case study in North China. *Science of the Total Environment, 631–632*, 348–357. https://doi.org/10.1016/j.scitotenv.2018.03.011

Maiz, I., Esnaola, M. V., & Millán, E. (1997). Evaluation of heavy metal availability in contaminated soils by a short sequential extraction procedure. *Science of the Total Environment, 206*(2–3), 107–115. https://doi.org/10.1016/S0048-9697(97)80002-2

Marco, A. D., Gentile, A. E., Arena, C., & Santo, A. D. (2005). Organic matter, nutrient content and biological activity in burned and unburned soils of a Mediterranean maquis area of southern Italy. *International Journal of Wildland Fire, 14*(4), 365–377. https://doi.org/10.1071/wf05030

McCutcheon, S. C., & Schnoor, J. L. (2003). Overview of phytotransformation and control of wastes. In *Phytoremediation: Transformation and control of contaminants* (3-58). John Wiley & Sons Inc.

Mickler, R. A., Earnhardt, T. S., & Moore, J. A. (2002). Regional estimation of current and future forest biomass. *Environmental Pollution, 116*, S7–S16. https://doi.org/10.1016/S0269-7491(01)00241-X

Miller, B., Dugwell, D. R., & Kandiyoti, R. (2003). The influence of injected HCl and SO_2 on the behavior of trace

elements during wood-bark combustion. *Energy & Fuels, 17*(5), 1382–1391. https://doi.org/10.1021/ef030020x

Moody, J. A., Kinner, D. A., & Úbeda, X. (2009). Linking hydraulic properties of fire-affected soils to infiltration and water repellency. *Journal of Hydrology, 379*(3–4), 291–303. https://doi.org/10.1016/j.jhydrol.2009.10.015

Muller, G. (1969). Index of geoaccumulation in sediments of the Rhine River. *GeoJournal, 2*, 108–118.

Murphy, S. F., McCleskey, R. B., Martin, D. A., Holloway, J. M., & Writer, J. H. (2020). Wildfire-driven changes in hydrology mobilize arsenic and metals from legacy mine waste. *Science of the Total Environment, 743*, 140635. https://doi.org/10.1016/j.scitotenv.2020.140635

Pearce, D. C., Dowling, K., & Sim, M. R. (2012). Cancer incidence and soil arsenic exposure in a historical gold mining area in Victoria, Australia: A geospatial analysis. *Journal of Exposure Science & Environmental Epidemiology, 22*(3), 248–257. https://doi.org/10.1038/jes.2012.15

Punjak, W. A., Uberoi, M., & Shadman, F. (1989). High-temperature adsorption of alkali vapors on solid sorbents. *AIChE Journal, 35*, 1186–1194. https://doi.org/10.1002/aic.690350714

Ranđelović, D., Gajić, G., Mutić, J., Pavlović, P., Mihailović, N., & Jovanović, S. (2016). Ecological potential of *Epilobium dodonaei* Vill. for restoration of metalliferous mine wastes. *Ecological Engineering, 95*, 800–810. https://doi.org/10.1016/j.ecoleng.2016.07.015

Rauret, G., López-Sánchez, J. F., Sahuquillo, A., Rubio, R., Davidson, C., Ure, A., & Quevauviller, P. (1999). Improvement of the BCR three step sequential extraction procedure prior to the certification of new sediment and soil reference materials. *Journal of Environmental Monitoring, 1*(1), 57–61. https://doi.org/10.1039/A807854H

Sánchez-Pinillos, M., De Cáceres, M., Casals, P., Alvarez, A., Beltrán, M., Pausas, J. G., Vayr-eda, J., & Coll, L. (2021). Spatial and temporal variations of overstory and understory fuels in Mediterranean landscapes. *Forest Ecology and Management, 490*, 119094. https://doi.org/10.1016/j.foreco.2021.119094

Shcherbov, B. L. (2012). The role of forest floor in migration of metals and artificial nuclides during forest fires in Siberia. *Contemporary Problems of Ecology, 5*(2), 191–199. https://doi.org/10.1134/S1995425512020114

Shin, H., Sidharthan, M., & Young, K. S. (2002). Forest fire ash impact on micro- and macroalgae in the receiving waters of the east coast of South Korea. *Marine Pollution Bulletin, 45*(1–12), 203–209. https://doi.org/10.1016/S0025-326X(02)00156-X

Sungur, A., Soylak, M., & Ozcan, H. (2014). Investigation of heavy metal mobility and availability by the BCR sequential extraction procedure: Relationship between soil properties and heavy metals availability. *Chemical Speciation & Bioavailability, 26*(4), 219–230. https://doi.org/10.3184/095422914X14147781158674

Ulery, A. L., Graham, R. C., & Amrhein, C. (1993). Wood-ash composition and soil pH following intense burning. *Soil Science, 156*(5), 358–364. https://doi.org/10.1097/00010694-199311000-00008

Xiaopin, Z., Bing, W., Shan, J., & Xuerong, D. (2010). The analysis for the calcium carbonate at high temperatures. *Guangdong Chemical Industry, 5*, 35.

Yao-Guo, W., You-Ning, X., & Zhang, J. H. (2010). Evaluation of ecological risk and primary empirical research on heavy metals in polluted soil over Xiaoqinling gold mining region, Shaanxi, China. *Transactions of Nonferrous Metals Society of China, 20*(4), 688–694. https://doi.org/10.1016/S1003-6326(09)60199-0

Young, D. R., & Jan, T. (1977). Fire fallout of metals off California. *Marine Pollution Bulletin, 8*(5), 109–112. https://doi.org/10.1016/0025-326X(77)90133-3

Yu, J., Sun, L., Wang, B., Qiao, Y., Xiang, J., Hu, S., Yao, H. (2016). Study on the behavior of heavy metals during thermal treatment of municipal solid waste (MSW) components. *Environmental Science & Pollution Research, 23*(1), 253–265. https://doi.org/10.1007/s11356-015-5644-7

Zhang, J., Xu, Y., Wu, Y., Hu, S., & Zhang, Y. (2019). Dynamic characteristics of heavy metal accumulation in the farmland soil over Xiaoqinling gold-mining region, Shaanxi, China. *Environmental Earth Sciences, 78*(1), 21–25. https://doi.org/10.1007/s12665-018-8013-2